Defect and Diffusion Forum
ISSN: 1662-9507, Vol. 385, pp 9-14
doi:10.4028/www.scientific.net/DDF.385.9

Submitted: 2018-02-16
Accepted: 2018-02-19
Online: 2018-07-20

Superplastic Flow and Micro-Mechanical Response of Ultrafine-Grained Materials

Megumi Kawasaki[1,a*], Jae-il Jang[2,b] and Terence G. Langdon[3,c]

[1]School of Mechanical, Industrial and Manufacturing Engineering, Oregon State University, Corvallis, OR 97330 U.S.A.

[2]Division of Materials Science, Hanyang University, Seoul, 04763, Republic of Korea

[3]Materials Research Group, Faculty of Engineering and the Environment, University of Southampton, Southampton SO17 1BJ, U.K.

[a]megumi.kawasaki@oregonstate.edu, [b]jijang@hanyang.ac.kr, [c]langdon@soton.ac.uk

Keywords: Nanoindentation, Severe plastic deformation, Strain rate sensitivity, Superplasticity, Ultrafine-grained materials

Abstract. The bulk ultrafine-grained (UFG) materials usually show superior mechanical properties. Since the occurrence of superplastic flow generally requires a grain size smaller than ~10 μm, it is anticipated that materials processed by severe plastic deformation (SPD) will exhibit superplastic ductilities when pulled in tension at elevated temperatures. Recent advances in the processing of UFG metals have provided an opportunity to extend the understanding of superplastic flow behavior to include UFG materials with submicrometer grain sizes. Recent studies showed the UFG materials demonstrated the development of plasticity in micro-mechanical response at room temperature by the significant changes in microstructure attributed to high-pressure torsion (HPT). Accordingly, this study summarizes recent results on excellent ductility and plasticity in a UFG Zn-22% Al alloy. Specifically, the alloy demonstrated the occurrence of exceptional superplastic flow at high temperature after equal-channel angular pressing and HPT and excellent room temperature plasticity of the alloy after HPT where the plasticity was evaluated by the nanoindentation technique. The significance of purity of the alloy is also considered for enhancing the ductility at room temperature.

Introduction

It is empirically defined that refinement in grain size improves both the strength and flow properties of polycrystalline metals. Accordingly, the development of severe plastic deformation (SPD) techniques was accelerated for fabricating ultrafine-grained (UFG) metals with grain sizes in the submicrometer and the nanometer ranges [1]. Processing by SPD introduces a very high imposed strain on a bulk solid without creating significant changes in the overall sample volume, and this is the way for the production of exceptional grain refinement. Various SPD techniques have been developed to produce UFG materials over the last two decades, but the most recognized procedures are equal-channel angular pressing (ECAP) [2] and high-pressure torsion (HPT) [3].

Superplastic elongations can be observed at elevated temperatures under conditions where the steady-state strain rate within the superplastic region, $\dot{\varepsilon}_{sp}$, is expressed by the following form [4]

$$\dot{\varepsilon}_{sp} = \frac{AD_{gb}G\mathbf{b}}{kT}\left(\frac{\mathbf{b}}{d}\right)^2\left(\frac{\sigma}{G}\right)^2 \quad (1)$$

where A is a dimensionless constant, D_{gb} is the coefficient for grain boundary diffusion, G is the shear modulus, $\mathbf{b}$ is the Burgers vector, k is Boltzmann's constant, T is the absolute temperature, d, is the grain size and σ is the flow stress. There are three important parameters for describing superplastic flow in Eq. (1). First, the exponent of the inverse grain size is given by $p = 2$. Second, the stress exponent is given by $n = 2$. Third, the temperature dependence is given by the diffusion coefficient for grain boundary diffusion so that the superplastic flow involves the activation energy for grain boundary diffusion, Q_{gb}.

On the contrary, room temperature (RT) plasticity can be evaluated by estimating the strain rate sensitivity, *m*. Since atomic diffusion is slow at ambient temperatures, grain boundary sliding is important for obtaining high ductility which can be evaluated by the value of *m*. Considering the empirical prediction where the flow stress, σ_f, is equivalent to a third of hardness, *H*/3, for fully plastic deformation at a constant strain rate, $\dot{\varepsilon}$, the value of *m* is determined by the expression [5]:

$$m = \left(\frac{\partial \ln \sigma_f}{\partial \ln \dot{\varepsilon}}\right)_{\varepsilon,T} = \left(\frac{\partial \ln (H/3)}{\partial \ln \dot{\varepsilon}}\right)_{\varepsilon,T} \quad (2)$$

Applying the empirical relation of $\dot{\varepsilon} = \dot{\varepsilon}_i \times 10^{-2} s^{-1}$ where $\dot{\varepsilon}_i$ is the indentation strain rate, Eq. (2) indicates that the value of *m* can be calculated from the slope of the line for each sample in a logarithmic plot of *H*/3 versus $\dot{\varepsilon}$.

Accordingly, this report was initiated to review the earlier experimental results and provide a comprehensive description of excellent ductility and plasticity in a UFG alloy processed by SPD techniques. Specifically, the following section describes the exceptional superplasticity observed at an elevated temperature in a Zn-22% Al alloy after ECAP and HPT and the results are evaluated in a deformation mechanism map. The next section describes the excellent RT plasticity of the HPT-processed Zn-22% Al alloy demonstrated by the nanoindentation technique.

Deformation Mechanism Maps for Depicting Superplastic Flow of UFG Metals

Examples of an excellent superplastic ductility were demonstrated in a Zn-22% Al eutectoid alloy after processing by ECAP for 8 passes at 473 K [6] and after processing by HPT for 5 turns at RT under an applied pressure of 6.0 GPa at a rotation speed of 1 rpm [7]. The tensile specimens machined after ECAP and HPT were deformed in tension at 473 K and the samples after failure are shown in Fig. 1 (a) and (b), respectively, where testing was conducted over a range of strain rates of 10^{-4} - 1.0 s^{-1} for the ECAP samples and 10^{-3} - 1.0 s^{-1} for the HPT samples.

Excellent superplastic flow was recorded with elongations up to 2230% at 10^{-2} s^{-1} after ECAP and a maximum of 1800% at 10^{-1} s^{-1} after HPT. This is due to significant grain refinement by the SPD processing to $d \approx 1.5$ μm after ECAP and ~610 nm after HPT in the alloy. Although a direct comparison is not adequate because of the different initial gauge dimensions, the alloy after the SPD processes demonstrated excellent superplasticity at 473 K. It is important to note that these optimal strain rates for superplastic ductilities are within the range of high strain rate superplasticity [8].

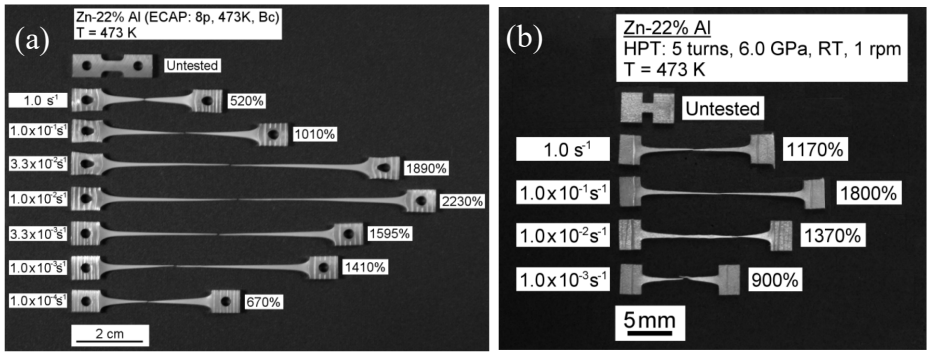

Fig. 1 Superplastic flow in a Zn-22% Al alloy after processing by (a) ECAP [6] and (b) HPT [7] and then testing at different strain rates at 473 K.

These sets of experimental data are evaluated by constructing a deformation mechanisms map using the format of $d/\mathbf{b}$ against σ/G at a constant testing temperature of 473 K so that in the theoretical approach a datum point showing superplastic flow appears in the area of the superplastic, Region II, expressed by Eq. (1). The constractured map is shown in Fig. 2 [7] where Regions I, II, and III denote the three regions of plastic flow associated with the Zn-22% Al alloy tested in an annealed condition before processing, and the fields for Nabarro–Herring and Coble diffusion creep are based on the theoretical models. The map includes a dashed line denoting the relationship of $d/\mathbf{b} = 20\ (\sigma/G)^{-1}$ which is defined experimentally that subgrains are formed under experimental testing conditions above the dashed line, thereby showing agreement with the field boundary between the superplastic Region II and Region III without superplasticity.

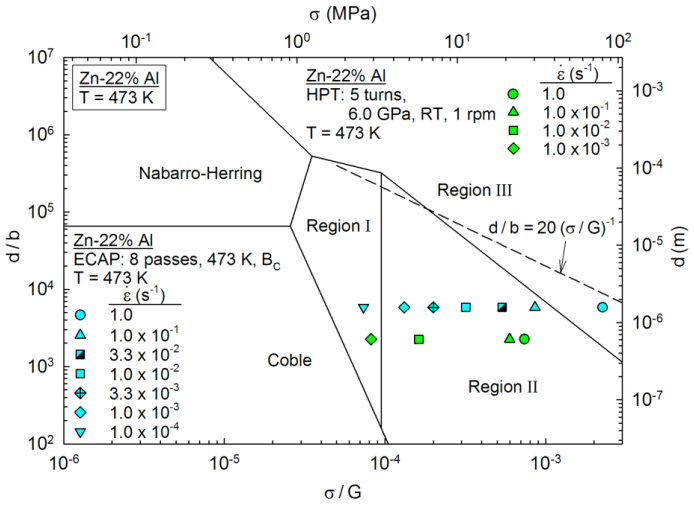

Fig. 2 A deformation mechanism map for a Zn-22% Al alloy tested at 473 K [7]: experimental points are for the samples processed by ECAP [6] and HPT [7].

The datum points for the ECAP and HPT samples are superimposed on the map in Fig. 2. It is apparent that, under a consistent testing temperature of 427 K, most datum points measured at intermediate strain rates are in Region II. On the contrary, the datum points falling outside the Region II are for the specimens tested at the slowest strain rates for both the ECAP and HPT specimens and the fastest strain rate for the ECAP sample where those failed to exhibit real superplasticity without necking within the deformed gauge lengths as seen in Fig. 1(a) and (b). Thus, it is reasonable to conclude that the superplastic flow of the Zn-22% Al alloy processed by both ECAP and HPT shows an excellent agreement with the deformation mechanism map based on the theoretical relationship for the rate of flow. Thereafter, the approach of evaluating the superplastic flow observed experimentally was demonstrated successfully by applying the theoretical equation for superplasticity in Eq. (1) for UFG materials after ECAP and HPT on Al and Mg alloys [9] and Al-Mg-Sc alloys after several different SPD and thermomechanical processing [10].

Excellent Plasticity at Room Temperature in a UFG Zn-Al Alloy

Processing by HPT was conducted at RT on the Zn-22% Al alloy under a compressive pressure of 6.0 GPa for 0, 1, 2 and 4 turns at 1 rpm where 0 turn denotes the sample in an as-annealed condition without processing. These samples are tested by the novel technique of nanoindentation at RT and the results are shown in Fig. 3 [11]. Specifically, Fig. 3(a) demonstrates the load-displacement curves recorded at four different indentation strain rates for the samples of 0 and 4 HPT turns and Fig. 3(b) shows the variation of the nanoindentation hardness, *H*, for the samples after HPT up to 4 turns tested at four different indentation rates [11].

An inspection in Fig. 2(a) shows the alloy both in an annealed condition without processing and after HPT demonstrates a strain rate dependency on the peak load displacements. From the nanoindentation hardness in Fig. 2(b), at all indentation strain rates the samples after HPT show significantly lower hardness by comparison with the sample before processing. In practice, the hardness decreases constantly with increasing numbers of HPT turns. Thus, the occurrence of strain weakening is observed in the Zn-22% Al alloy after HPT up to 4 passes, rather than strengthening due to grain refinement after processing. Thus, the reason for this strain softening in the Zn-Al alloy is not due to conventional strain softening caused by recrystallization of the material.

This unique behavior may occur extensively as a result of severe imposed pressure during processing. In practice, this can be explained by earlier studies where transmission electron microscopy (TEM) observed that the hard Zn precipitates in Al-rich grains are absorbed within the Zn-rich grains during severe straining by ECAP [12] and HPT [13]. Thus, precipitation strengthening by Zn is lowered during severe plastic deformation that results in the weakening of the material with increasing imposed strain.

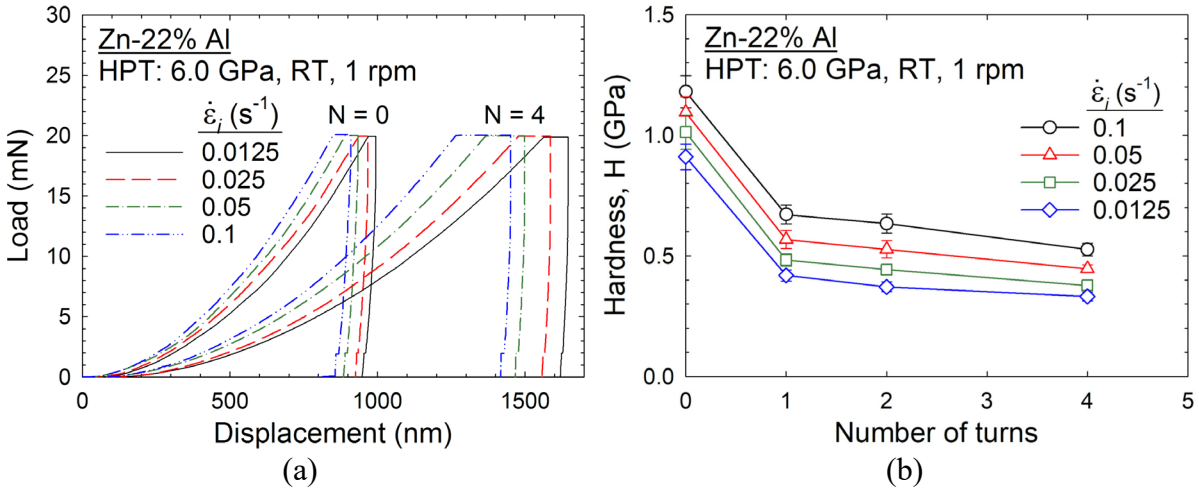

Fig. 3 (a) Representative load-displacement curves taken at four different indentation rates for the Zn-22% Zn alloy disks after HPT for 0 and 4 turns and (b) variation of hardness, H, with increasing numbers of HPT turns up to 4 [11].

In order to evaluate the plasticity at RT in the Zn-Al alloy after HPT, the essential material property of strain rate sensitivity was estimated and the results are shown in Fig. 4 from the series of nanoindentation data including the results in Fig. 3(a). It is apparent that the estimated *m* values after HPT processing were significantly higher than for the sample without processing, thereby confirming the trend of enhanced plasticity by HPT. The high values of *m* after HPT processing are in excellent agreement with the earlier reports demonstrating *m* values of ~0.25 and ~0.30 for a Zn-22% Al alloy after ECAP through 4 passes [14,15] and 8 passes [15], respectively, under conventional tensile testing at strain rates of ~10^{-4} – 10^{-2} s^{-1}.

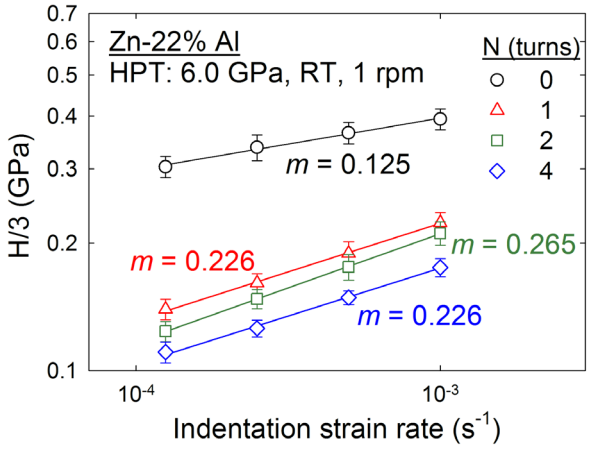

Fig. 4 Variation of the values of m for the Zn-Al alloy before and after HPT for different numbers of turns. The m values were estimated as the slope of the line in the logarithmic plot of estimated flow stress versus indentation strain rates. [11]

From the early literature, it is well defined that superplastic ductility refers to exceptionally high elongations of at least 400% without necking when testing in tension at elevated temperatures of $T \geq 0.5T_m$ (T_m: the absolute melting temperature) [16]. In conventional superplastic metals including Zn-22% Al alloy, as seen in Eq. (1), the plastic flow within the superplastic regime occurs by grain boundary sliding. Thereby, because of the low T_m of the Zn-Al eutectoid alloy where RT corresponds to ~$0.44T_m$, the alloy demonstrates very high values of *m* implying excellent plasticity at RT by the dominant deformation mechanism of grain boundary sliding. The variation in *m* with increasing HPT turns is related to the capability of grain boundary sliding influenced by the homogeneous distribution of the Zn and Al phases with increasing torsional straining by HPT [9]. Nevertheless, the results revealed superior plasticity at RT in the Zn-Al alloy after HPT.

It is worth noting the significance of applying the novel nanoindentation technique on to SPD-processed materials. The main benefit relates to the requirement of limited volume for each measurement. It is especially favorable for relatively small samples processed by HPT in the current laboratory-scale studies. The nanoindentation tests allow examinations at arbitrarily selected local points within a sample so that a series of mechanical properties can be examined at a local point in a gradient-type microstructure which is often observed after HPT. A very recent review examined and summarized the available experimental results showing the enhancement in strength and plasticity in terms of the micro-mechanical behavior at RT in a range of metals and alloys processed by several different SPD processing procedures [17].

Finally, it is important to note that impurities in UFG materials significantly influence the ductility at ambient temperatures. A recent study carefully prepared a series of a Zn-22% Al alloy with different Si impurity contents of <10 to 1500 ppm within an homogeneous distribution of Zn and Al grains with an average grain size of ~0.63 through thermo-mechanical processing [18]. Tensile testing at RT demonstrated the occurrence of excellent RT superplasticity in the high-purity Zn-Al alloy with a maximum elongation of >500 % at a strain rate of 1.0×10^{-3} s^{-1} where in fact the recorded elongation is one of the highest RT superplastic elongations to date in Zn-22 % Al alloys. The variation of elongation to failure for the series of the Zn-Al samples with different impurity contents are shown in Fig. 5 [18]. It is apparent that increasing Si contents decreases the elongation to failure at the optimal superplastic strain rate of 1.0×10^{-3} s^{-1} at RT in the alloy. A detailed analysis on fractography after superplastic flow demonstrated that the difference in Si content did not influence the deformation mechanism but affected the fracture mode of the Zn-Al alloy. Thus, the production of bulk metals with submicrometer grain sizes advances the opportunity to demonstrate improved mechanical properties including both high strength and ductility, but careful material preparation may significantly enhance the ultimate properties of UFG materials.

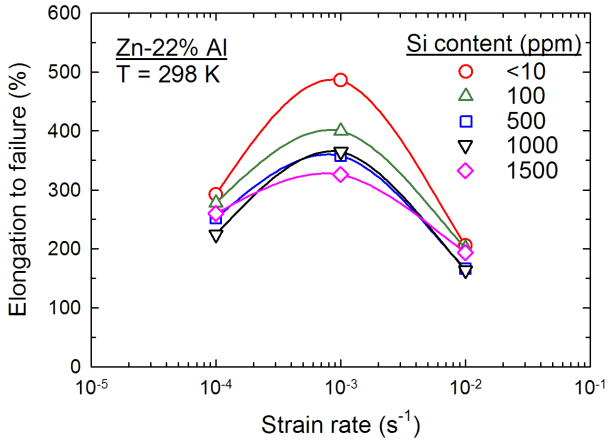

Fig. 5 Variations of elongation to failure for the Zn-22% Al alloy with different Si contents tested at 298 K at three different strain rates [18].

Summary

This report summarizes the recent results on a UFG Zn-22%Al alloy after ECAP and HPT showing excellent superplastic ductility at elevated temperature and high plasticity at room temperature examined by nanoindentation testing. Over this wide temperature range, the submicrometer grains accelerate the level of grain boundary sliding leading to high ductility and plasticity in the Zn-Al alloy. Further grain refinement as well as careful materials preparation may even enhance the ductility of UFG materials over a wide range of testing temperatures.

Acknowledgements

This work was supported by the NRF Korea funded by MSIP under Grant No. NRF-2015R1A5A1037627 and NRF-2017R1A2B4012255 (JIJ); and the European Research Council under ERC Grant Agreement No. 267464-SPDMETALS (TGL).

References

[1] R.Z. Valiev, Y. Estrin, Z. Horita, T.G. Langdon, M.J. Zehetbauer, Y.T. Zhu, Producing bulk ultrafine-grained materials by severe plastic deformation, 58(4) JOM (2006) 33-39.

[2] R.Z. Valiev, T.G. Langdon, Principles of equal-channel angular pressing as a processing tool for grain refinement, Prog. Mater. Sci. 51 (2006) 881-981.

[3] A. P. Zhilyaev, T. G. Langdon, Using high-pressure torsion for metal processing: Fundamentals and applications, Prog. Mater. Sci. 53 (2008) 893-979.

[4] T.G. Langdon, A unified approach to grain boundary sliding in creep and superplasticity, Acta Metall. Mater. 42 (1994) 2437-2443.

[5] S. Shim, J.-i. Jang, G.M. Pharr, Extraction of flow properties of single-crystal silicon carbide by nanoindentation and finite-element simulation, Acta Mater. 56 (2008) 3824-3832.

[6] M. Kawasaki, T.G. Langdon, Grain boundary sliding in a superplastic zinc-aluminum alloy processed using severe plastic deformation, Mater. Trans. 49 (2008) 84-89.

[7] M. Kawasaki, T.G. Langdon, Developing superplasticity and a deformation mechanism map for the Zn–Al eutectoid alloy processed by high-pressure torsion, Mater. Sci. Eng. A 528 (2011) 6140-6145.

[8] K. Higashi, M. Mabuchi, T.G. Langdon, High-strain-rate superplasticity in metallic materials and the potential for ceramic materials, ISIJ Intl. 36 (1996) 1423-1438.

[9] M. Kawasaki, T.G. Langdon, Review: achieving superplastic properties in ultrafine-grained materials at high temperatures, J. Mater. Sci. 51 (2016) 19–32.

[10] P.H.R. Pereira, Y. Huang, M. Kawasaki, T.G. Langdon, An examination of the superplastic characteristics of Al–Mg–Sc, alloys after processing, J. Mater. Res. 22 (2017) 4541-4553.

[11] I.-C. Choi, Y.-J. Kim, B. Ahn, M. Kawasaki, T.G. Langdon, J.-I. Jang, Evolution of plasticity, strain-rate sensitivity and the underlying deformation mechanism in Zn-22% Al during high-pressure torsion, Scripta Mater. 75 (2014) 102-105.

[12] M. Furukawa, Z. Horita, M. Nemoto, R.Z. Valiev, T.G. Langdon, Fabrication of submicrometer-grained Zn-22% Al by torsion straining, J. Mater. Res. 11 (1996) 2128-2130.

[13] M. Furukawa, Y. Ma, Z. Horita, M. Nemoto, R.Z. Valiev, T.G. Langdon, Microstructural characteristics and superplastic ductility in a Zn-22% Al alloy with submicrometer grain size, Mater. Sci. Eng. A241 (1998) 122-128.

[14] T. Tanaka, H. Watanabe, M. Kohzu, K. Higashi, Microstructure and superplastic properties at room temperature in Zn-22Al alloy after equal-channel-angular extrusion, Mater. Sci. Forum 447-448 (2004) 489-496.

[15] P. Kumar, C. Xu, T.G. Langdon, The significance of grain boundary sliding in the superplastic Zn–22% Al alloy after processing by ECAP, Mater. Sci. Eng. A 410–411 (2005) 447-450.

[16] T.G. Langdon, Seventy-five years of superplasticity: historic developments and new opportunities, J. Mater. Sci. 44 (2009) 5998-6010.

[17] M. Kawasaki, B. Ahn, P. Kumar, J.-i. Jang, T.G. Langdon, Nano- and micro-mechanical properties of ultrafine-grained materials processed by severe plastic deformation techniques, Adv. Eng. Mater. 19 (2017) 1600578(1-17).

[18] T. Uesugi, M. Kawasaki, M. Ninomiya, Y. Kamiya, Y. Takigawa, K. Higashi, Significance of Si impurities on exceptional room-temperature superplasticity in a high-purity Zn-22%-Al alloy, Mater. Sci. Eng. A 645 (2015) 47-56.